Formation processes of basal ice at Hamna Glacier, Sôya Coast, East Antarctica, inferred by detailed co-isotopic analyses

Yoshinori Iizuka,[1*] Hiroshi Satake,[2] Takayuki Shiraiwa,[1] Renji Naruse[1]
[1]*Institute of Low Temperature Science, Hokkaido University, Sapporo, Hokkaido 060-0819, Japan*
[2]*Department of Environmental Chemistry and Biology, Toyama University, Toyama 930-0887, Japan*

ABSTRACT. Debris-laden basal ice is exposed along an ice cliff near Hamna Glacier, Sôya Coast, East Antarctica. The basal ice is about 6.8 m thick and shows conspicuous stratigraphic features. The upper 5.5 m consists of alternating layers of bubble-free and bubbly ice. δ values of the bubble-free ice layers are enriched by 2.4 ± 1.0‰ (standard deviation) for δ^{18}O compared to values of neighboring bubbly ice layers above, and slopes of δ^{18}O vs δD are close to 8. Such layers are suggested to have been formed by refreezing of meltwater in an open system. In contrast, part of the bubbly ice layers shows neutral profiles for stable isotopes, suggesting that these ice masses are undisturbed ice-sheet ice which was not affected by melting and freezing. The massive alternating layers are thus considered to have been formed by folding of refrozen and non-melted layers. The lower 1.3 m consists predominantly of bubble-free massive ice. The profile of co-isotopic values shows a change of about 3.0‰ for δ^{18}O at the interface between bubble-free and bubbly ice. Since the isotopic change occurred over a wider thickness than the upper 5.5 m, the basal ice is suggested to have been formed by refreezing of meltwater on a larger scale than the upper 5.5 m.

INTRODUCTION

The basal ice of glaciers and ice sheets has been widely studied to understand the inaccessible ice–bed interface (e.g. Gow and others, 1979; Lawson, 1979; Knight, 1994; Hubbard and Sharp, 1995). Various formation processes of the basal ice have been proposed from various types of glaciers and ice sheets: shear (Tison and others, 1993), regelation (Weertman, 1964), congelation related to change in the basal thermal regime (Knight, 1987) and freezing of supercooled water (Lawson and others, 1998). The processes change from one glacier to another, or even from one part to another within the same glacier. In East Antarctica there have been only a few studies of basal ice (Goodwin, 1993; Tison and others, 1993; Fitzsimons, 1996; Bouzette and Souchez, 1999; Kluiving and others, 1999), and these have proposed different formation processes in each region.

Stable-isotopic analysis is one of the most promising techniques used to study the basal ice. Co-isotopic analyses based on δ^{18}O and δD are especially useful since they reveal not only the possibility of liquid-water existence (Jouzel and Souchez, 1982) but also the refreezing condition at the base of glaciers and ice sheets (Souchez and Jouzel, 1984; Souchez and de Groote, 1985). However, the technique has been applied solely to bulk measurements of the basal ice. Such studies have either discussed bulk processes of refreezing or compared bulk isotopic values of basal ice and those of meteoric glacier ice on the basis of slopes of δ^{18}O vs δD diagrams (e.g. Sugden and others, 1987; Zdanowicz and others, 1996; Lawson and others, 1998). It is unlikely, however, that basal ice several meters thick could be formed by one refreezing cycle. More detailed treatment of the basal ice is necessary to detect single freezing events in basal ice.

In contrast to the analyses of basal ice from glaciers and ice sheets, past theoretical and experimental isotopic studies of this problem describe the single-event melting and refreezing process (Jouzel and Souchez, 1982; Souchez and Jouzel, 1984; Souchez and others, 1987; Lehmann and Siegenthaler, 1991). Theoretical studies of formation processes of basal ice have also considered a single refreezing process (e.g. Weertman, 1964; Robin, 1976; Lliboutry, 1993; Alley and others, 1998). In order to compare the theoretical and experimental results so far obtained, isotopic analyses of ice from glaciers and ice sheets should be performed for a single refreezing process. Jansson and others (1996) presented a study with this goal. However, their rough sampling interval (15 mm) prevented them from discussing the refreezing process at the base of the glacier. Multiple isotopic values from a single refrozen ice layer are needed to investigate the refreezing process at the base by curve-fitting for ice samples on δ^{18}O vs δD diagrams.

In this paper, we present a detailed co-isotopic study from the basal ice of Hamna Glacier, Dronning Maud Land, East Antarctica. Vertical profiles formed by basal ice samples on δ^{18}O and δD were used to deduce the processes occurring beneath the East Antarctic ice sheet on the basis of past theoretical and experimental studies.

* Present address: National Institute of Polar Research, Tokyo 173-8515, Japan.

https://doi.org/10.3189/172756501781832359 Published online by Cambridge University Press

STUDY SITE AND ANALYTICAL PROCEDURES

The sampling site is located on the left bank of Hamna Glacier, one of the outlet glaciers from the East Antarctic ice sheet, 30 km south of Syowa station, Sôya Coast, Dronning Maud Land (Fig. 1). The figure shows the ice sheet to the southeast and a bedrock hill to the northwest whose summit is 141 m a.s.l.

The terminus of Hamna Glacier forms an ice cliff about 30 m high. The lower part of the ice cliff is an exposed debris-laden basal ice layer 6.8 m thick (hereafter called Hamna Basal Ice; Fig. 2). The sequence of the basal layer extends laterally, without any stratigraphic disturbances, for more than 500 m from the sampling site to an ice-marginal lake to the west. The debris has probably originated from subglacial bedrock, since there are no nunataks on the upper reaches of Hamna Glacier. The basal ice is considered to have preserved features formed in the inland area in the Sôya drainage basin, because outflow of water due to basal melting has not been observed in this area. The basal ice is composed of two parts: the upper stratified bubble-free and bubbly layers, and the lower massive bubble-free layer containing several debris-rich horizons. The lower layer rests directly on the crystalline basement rock. Above the basal ice, we observed white bubble-rich ice to the top of the ice cliff. Since there is no indication of visible disturbance in this ice, we consider it ordinary ice-sheet ice.

The basal ice was sampled in winter 1994 during the 35th Japanese Antarctic Research Expedition. Using a chain-saw, a columnar section was cut from the ice cliff. It covers the lower 9 m of the cliff, so the sample includes not only the Hamna Basal Ice but also the upper undisturbed ice-sheet ice. The samples were transported frozen to a cold laboratory in the Institute of Low Temperature Science, Sapporo, Japan, and preserved there at −20°C.

Two kinds of laboratory analyses, which have different measurement intervals for isotope analysis, were conducted. The first was a general analysis of the entire basal ice layer. Analyses included stratigraphy, ice-crystal orientation, debris concentration (percentage in weight) and stable isotopes ($\delta^{18}O$ and δD). Stable-isotopic analyses were performed continuously every 100 mm in thickness. The second was a detailed analysis focusing on particular stratigraphic sections. Several characteristic parts about 100–200 mm long were used for detailed stable-isotopic analyses, which were done every 1.5–5 mm in thickness. Isotope analyses were carried out with a mass spectrometer (PRISM) at Toyama University, Japan. The CO_2- and H_2-water equilibration method was

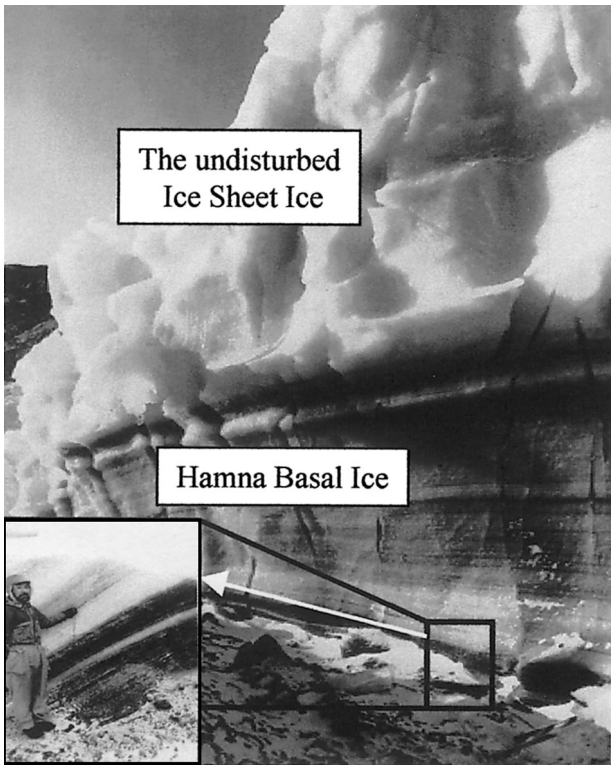

Fig. 2. Sampling site of Hamna Basal Ice used for analyses. This ice cliff is about 30 m high, and debris-laden ice (basal ice) is about 6.8 m in thickness. The basal ice and the upper white ice of the cliff were sampled continuously through 9 m in thickness. Black ice layers in the photograph contain less debris and few bubbles. The small picture at lower left shows a close-up view of the lower part of the Hamna Basal Ice which looks more black. The white arrow shows the interface between the upper and lower parts of the Hamna Basal Ice.

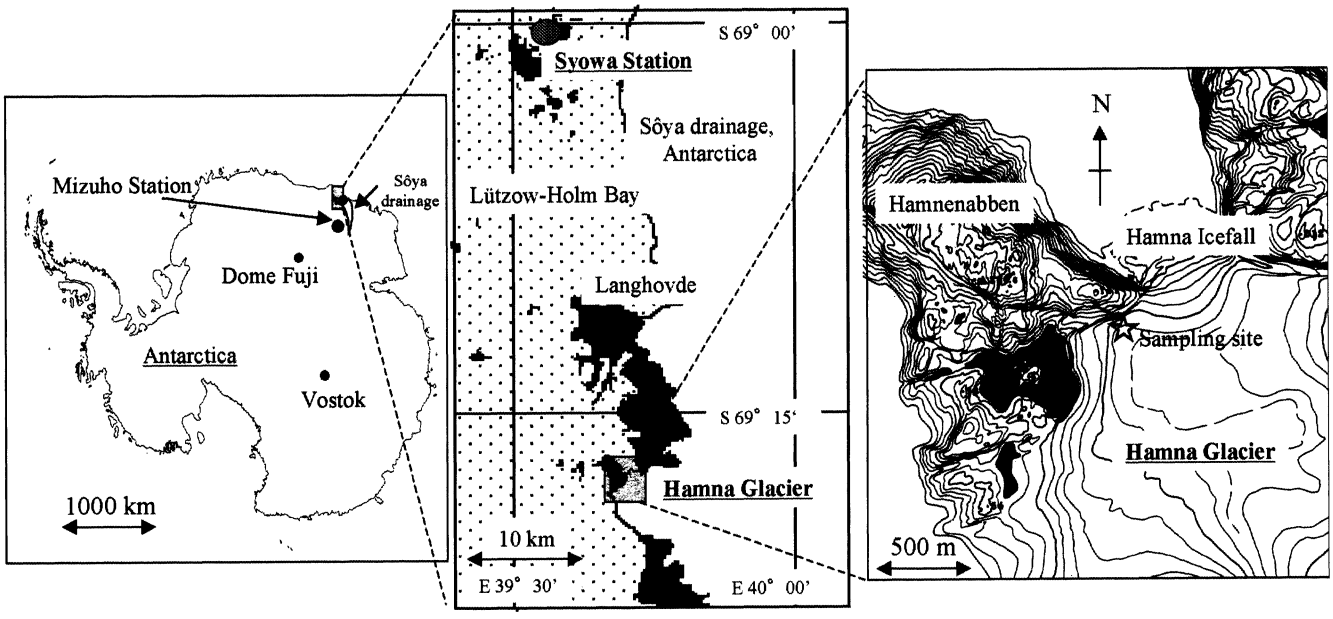

Fig. 1. Location map of the Hamna Basal Ice. It is exposed at the east coast of the Sôya drainage in East Antarctica. The sampling site is shown as ☆ in the close-up view.

https://doi.org/10.3189/172756501781832359 Published online by Cambridge University Press

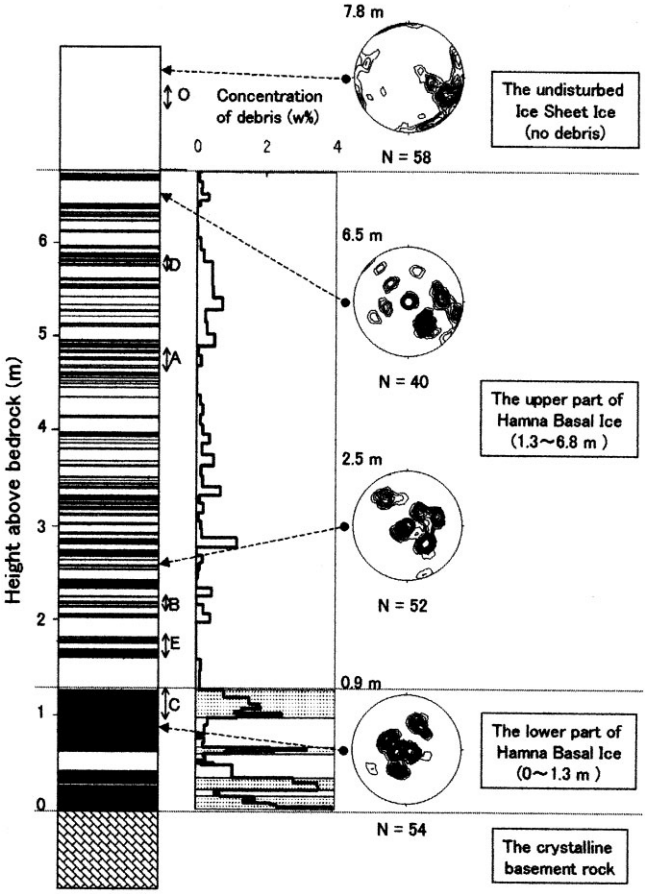

Fig. 3. Stratigraphy, debris concentration and ice fabrics of the Hamna Basal Ice. Bubbly ice is represented by open spaces, and bubble-free ice by black spaces, in the left column. Debris layers shown by dotted spaces in the right column are composed of bubble-free ice. Schmidt plots of the c axis of the basal ice and the upper ice-sheet ice are shown at four heights on the right. The c axis was measured, using a Universal Stage, from thin parallel sections cut in the layers of bubbly or bubble-free ice. Numbers show heights on the ice cliff. Symbols on the right side of the left column show samples used for isotopic analyses. O, A, B and C denote the Ice Sheet Ice and Basal Ice-A, -B and -C in Figure 6, D the Basal Ice-D in Figure 7, and E the Basal Ice-E in Figure 8.

adopted for the measurement of isotopic ratios using a Pt catalyst for H_2-water (Ohba and Hirabayashi, 1996). Analyses of δD were performed twice for each sample, and means of two measurements are given. Errors are estimated to be less than ±0.1‰ for δ^{18}O, and ±1.4‰ for δD (1σ error).

RESULTS

Figure 3 shows the entire stratigraphy of bubbly ice, bubble-free ice and debris layers observed on the Hamna Basal Ice, together with the debris concentration in each layer. The vertical axis represents height measured upward from the base of the ice sheet. Hereafter, we take the height in this way. The Hamna Basal Ice exhibits two peculiar stratigraphic features. The upper part of the basal ice (height: 1.3–6.8 m) consists of alternating layers of bubble-free and bubbly ice of order mm to cm in thickness and has low concentration (<1% in weight) of debris. The lower part of the basal ice (height: 0–1.3 m) consists predominantly of bubble-free ice and has high concentration (up to 4% in weight) of debris. The stratigraphic features

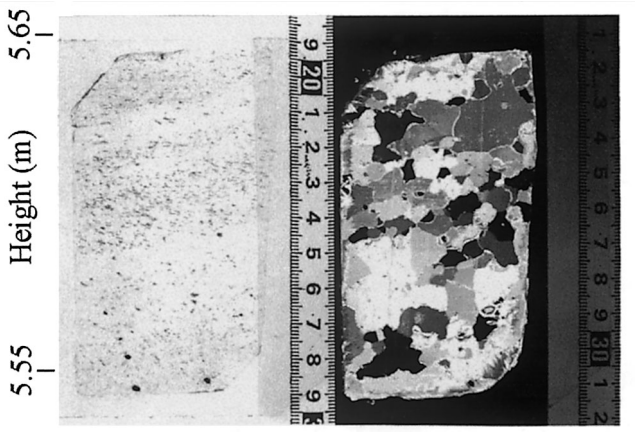

Fig. 4. Thin-section photograph of alternating layers at about 5.6 m in height. The left photograph was taken by transmitted light, and the existence of bubbles in ice can be seen. The right photograph was by polarized light, and crystal diameters can be measured.

of the upper part are described by contemporary terminology such as dispersed facies (Lawson, 1979), clotted ice (Knight, 1987) and clear or laminated facies (Hubbard and Sharp, 1995). Features of the lower part are classified as stratified facies (Lawson, 1979; Hubbard and Sharp, 1995) and stratified or debris-banded facies (Knight, 1987).

Figure 3 also shows Schmidt plots of the *c*-axis orientation of the basal ice and the upper ice-sheet ice. Ice fabrics of Hamna Basal Ice (0.9, 2.5 and 6.5 m high) have different patterns from that of the overlying ice-sheet ice (7.8 m high), which shows an ambiguous single-maximum pattern. The upper and lower parts of the basal ice have a similar pattern of multiple-maximum fabrics. Kizaki (1962) proved that such multiple-maximum fabrics can be produced by ice being subjected to long-continued strain under strong shear stress.

Figure 4 shows photographs of a thin section of the upper part at about 5.6 m height. The stratification formed by different air-bubble concentrations in the transparent figures corresponds to the difference in crystal size in the cross-polarized figure. Table 1 shows statistical values of crystal size observed in the thin sections. The average diameter of the ice crystals in the bubble-free ice layers is one and a half times larger than that in the bubbly ice layers.

A bulk measurement of stable isotopes of the basal ice is shown in Figure 5. Both δ^{18}O and δD show lower values (−45.6‰ and −364‰ on average, respectively) than precipitation in the marginal region of the Sôya drainage basin where seasonal δ^{18}O values range from −33‰ to −10‰ at present (Kato, 1979). The result indicates that the basal ice originated from precipitation in inland regions of the ice sheet. If we assume that the present spatial distribution of δ^{18}O values in the Sôya drainage basin (Satow and Watanabe, 1992) does not change, the Hamna Basal Ice

Table 1. Crystal sizes in the thin section shown in Figure 4

	Longest axis	*Normal axis to the longest axis*
	mm	mm
All crystals (n = 117)	9.0 ± 6.8	5.2 ± 3.9
Crystals of bubbly ice (n = 86)	7.9 ± 5.6	4.6 ± 3.1
Crystals of bubble-free-ice (n = 31)	12.1 ± 9.2	6.9 ± 5.7

https://doi.org/10.3189/172756501781832359 Published online by Cambridge University Press

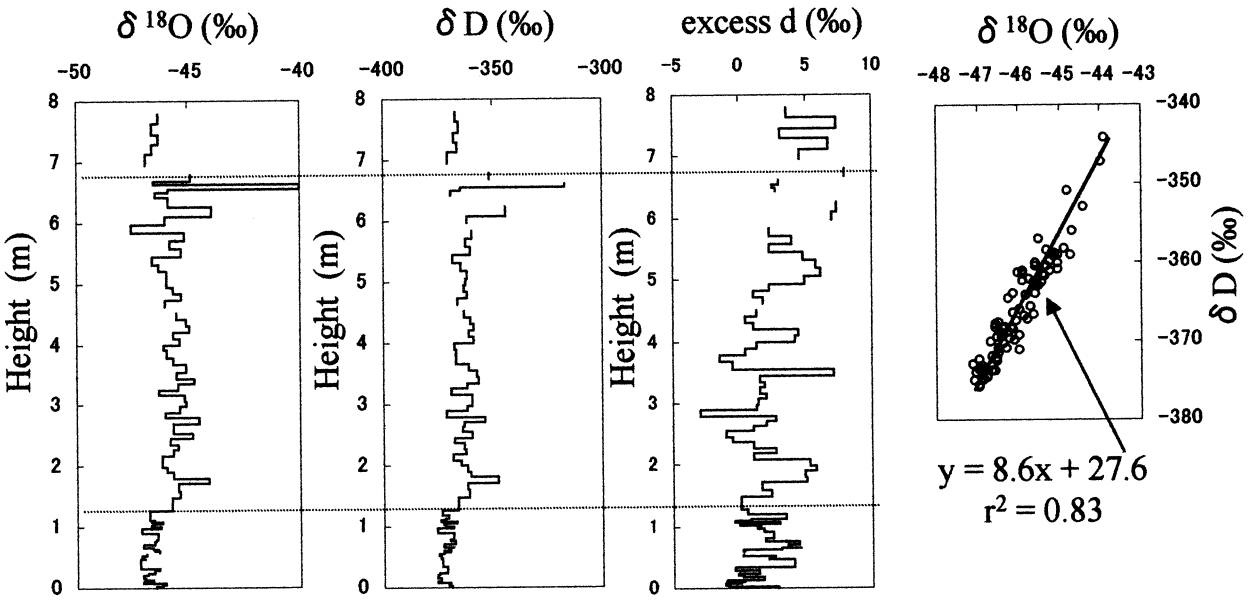

Fig. 5. Bulk vertical distributions of $\delta^{18}O$ (‰), δD (‰) and deuterium excess d (‰; $= \delta D - 8\times \delta^{18}O$) in Hamna Basal Ice. The dotted lines are dividing lines between the ice-sheet ice and the upper part, and between the upper and lower parts. The rightmost panel shows a co-isotopic plot for the whole basal ice mass. This plot omits the samples at about 6.6 m, because an inaccurate correlation coefficient of the co-isotopic plot is introduced due to much heavier δ values at about 6.6 m than for the other samples. The number of samples taken from the plot is 82.

could have originated from precipitation in the inland area around 3000 m a.s.l., about 150 km southeast from Mizuho station (70°42′ S, 44°20′ E). The excess *d* value (2‰ on average) is lower than the value for the ice-sheet ice (5‰ on average) or meteoric line (10‰; Craig, 1961).

In order to examine the formation mechanism of the alternating layers, we selected four particular parts, each 100–200 mm thick, for detailed isotopic analyses in which the sampling interval is 5 mm. One of these was selected from the upper undisturbed ice-sheet ice above the basal ice (Ice Sheet Ice), two were from the upper part of the basal ice (Basal Ice-A and -B), and one was from the lower part (Basal Ice-C). Only Basal Ice-A and -B have the alternating layers. Stratigraphy and vertical distributions of $\delta^{18}O$ and δD in the four parts are shown in Figure 6. In order to acquire more detailed information, we selected two particular parts in the upper part of the basal ice: one is about 100 mm thick with sampling resolution of 3 mm (Basal Ice-D), and the other is about 200 mm thick with sampling resolution of 1.5 mm (Basal Ice-E). Basal Ice-D and -E also have alternating layers. Stratigraphy and vertical distributions of $\delta^{18}O$ in Basal Ice-D and -E are shown in Figures 7 and 8.

δ values in the Ice Sheet Ice and in Basal Ice-A, -B, -C, -D and -E are the same as in the bulk measurements plotted in Figure 5, ranging from −47‰ to −40‰ for $\delta^{18}O$, and −380‰ to −320‰ for δD. But $\delta^{18}O$ and δD vertical profiles between

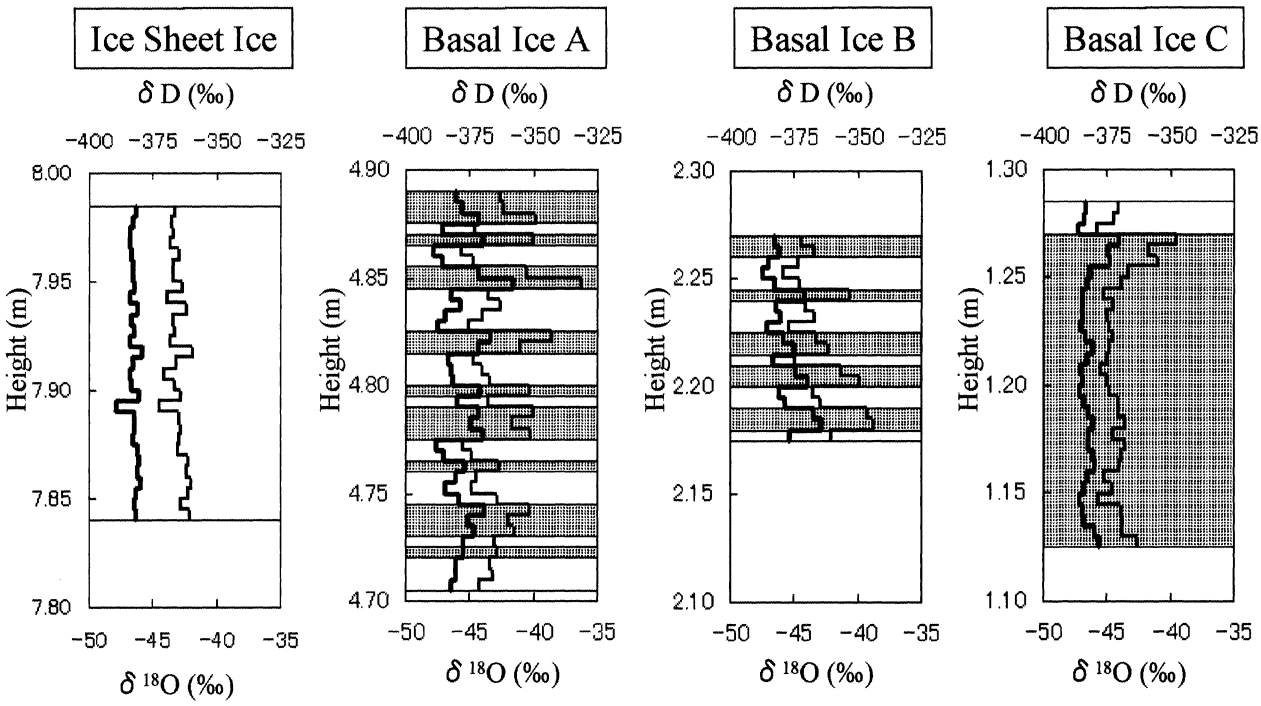

Fig. 6. Vertical profiles of $\delta^{18}O$ and δD values at four locations in the Hamna ice cliff. Thick lines represent $\delta^{18}O$ (‰), and thin lines δD (‰). Dotted and open squares show bubble-free ice and bubbly ice, respectively. The vertical axis represents the height (m).

https://doi.org/10.3189/172756501781832359 Published online by Cambridge University Press

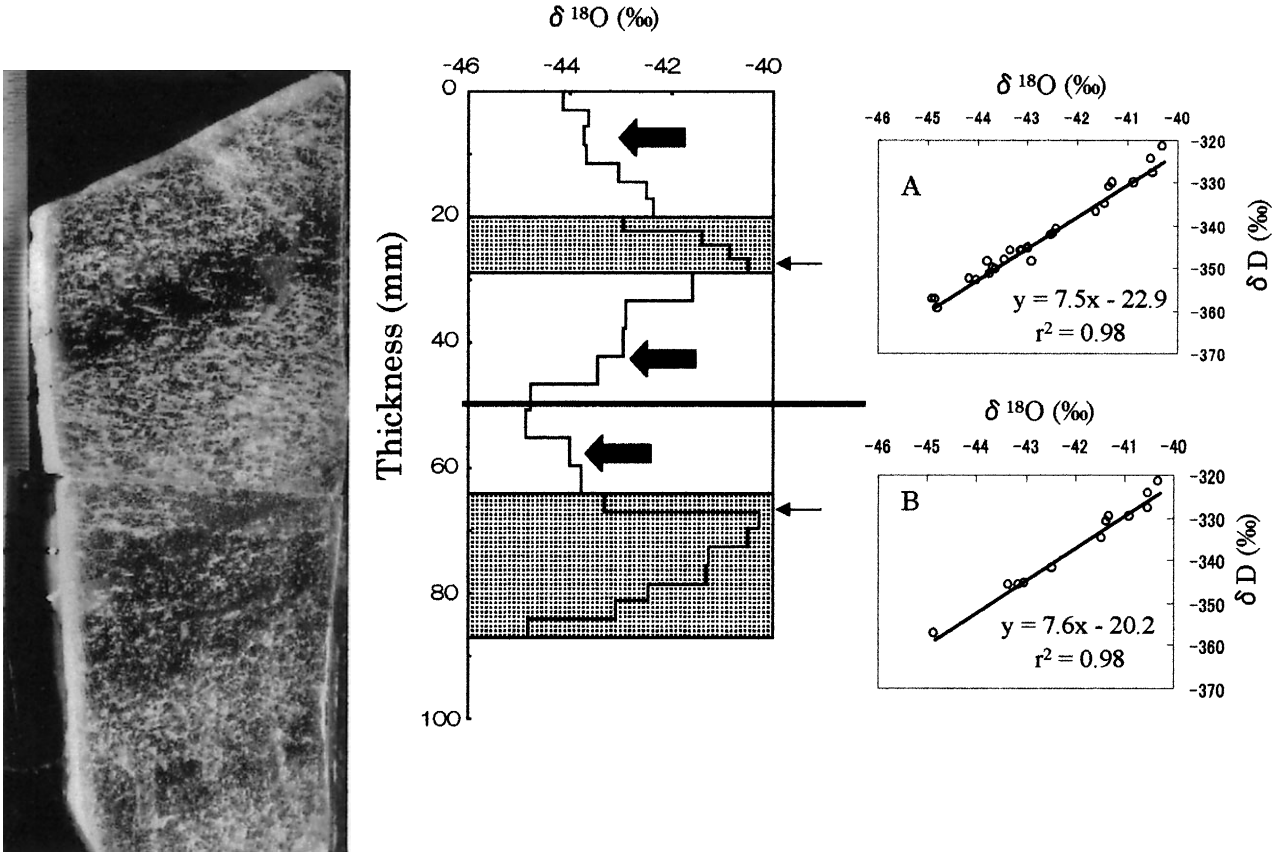

Fig. 7. A photograph and a vertical profile of $\delta^{18}O$ (‰) values of Basal Ice-D at about 5.8 m in height. Dotted and open squares show bubble-free ice and bubbly ice layers, respectively. The vertical axis represents the thickness (mm). Each value was measured through about a 3 mm thickness. Thin arrows show maximum values of the isotopic profile. Thick black arrows show the bubbly ice layers whose isotopic fluctuation is decreasing from neighboring bubble-free ice. Slopes of $\delta^{18}O$ vs δD of all the samples (A: 27 samples) and of samples on the bubble-free ice (B: 12 samples) are also shown.

the Ice Sheet Ice and Basal Ice-A, -B, -C, -D and -E have different patterns. Variations in $\delta^{18}O$ and δD values in the Ice Sheet Ice are so small (<2.2‰ and 13‰ for $\delta^{18}O$ and δD, respectively) that it is difficult to find any features caused by seasonal or climatic changes in δ values of precipitation. On the other hand, variations in the Basal Ice-A, -B, -C, -D and -E are large, as much as 6.0‰ and 50‰, for $\delta^{18}O$ and δD, respectively.

Isotopic curves of Basal Ice-A, -B, -D and -E, which belong to the upper part of the basal ice, are closely related to the alternating layers of bubble-free and bubbly ice. In each alternating layer, almost all the δ values of the bubble-free ice layers are heavier than those of the neighboring bubbly ice layers. The average values of isotopic fluctuations between the bubble-free and the neighboring bubbly ice layers observed in Basal Ice-A and -B are 2.4 ± 1.0‰ (standard deviation) and 19 ± 8‰ for $\delta^{18}O$ and δD, respectively. In the cases of Basal Ice-D and -E, the average differences defined by the maxima in the bubble-free ice layers and minima in the neighboring bubbly ice layers are 2.6 ± 1.2 (standard deviation) and 21 ± 9‰ for $\delta^{18}O$ and δD. In some cases, they are enriched by 5–6‰ for $\delta^{18}O$ and by 45–50‰ for δD (e.g. at 4.86 m in Basal Ice-A and at 40 mm in Basal Ice-E shown in Figs 6 and 8).

The co-isotopic profile of Basal Ice-C, which belongs to the lower part of the basal ice, shows that a sudden isotopic change (3.2‰ and 30‰ for $\delta^{18}O$ and δD, respectively) occurs at the boundary between the bubble-free and bubbly ice layers, and δ values decrease downward with height in the bubble-free ice. Values of excess *d* of Basal Ice-A, -B, -C, -D and -E are similar to the values of the whole basal ice (2‰ on average), and fluctuations of excess *d* are unrelated to the stratigraphy of bubbles.

DISCUSSION

Formation processes of bubble-free and bubbly ice layers in the upper part of the Hamna Basal Ice

The isotopic variations found in the upper part of Basal Ice-A, -B, -D and -E (Figs 6–8) are suggested to have been formed when the alternating layers of bubble-free and bubbly ice were created at the base in the inland Sôya drainage basin. This idea is justified first by the fact that significant variations in stable isotopes were not observed in the undisturbed bubbly ice overlying the Hamna Basal Ice (Ice Sheet Ice in Fig. 6). Second, the bubble-free layers exist only in the basal ice. Third, the isotopic variations correspond closely to the alternating layers.

Stable isotopes have been used as an indicator of phase change in H_2O (e.g. Jouzel and Souchez, 1982). Theoretical considerations show that freezing of water induces isotopic enrichment of 3.0‰ for $\delta^{18}O$ and 18.7‰ for δD (O'Neil, 1968) from initial water to ice formed by freezing of the water for the first time. In alternating layers in the upper part of the Hamna Basal Ice, similar variations in δ values were found; heavier δ values of 2.4 ± 1.0‰ and 19 ± 8‰ for $\delta^{18}O$ and δD were observed in the bubble-free ice layers as compared with the neighboring bubbly ice layers. This suggests that the bubble-free layers in the upper part were

https://doi.org/10.3189/172756501781832359 Published online by Cambridge University Press

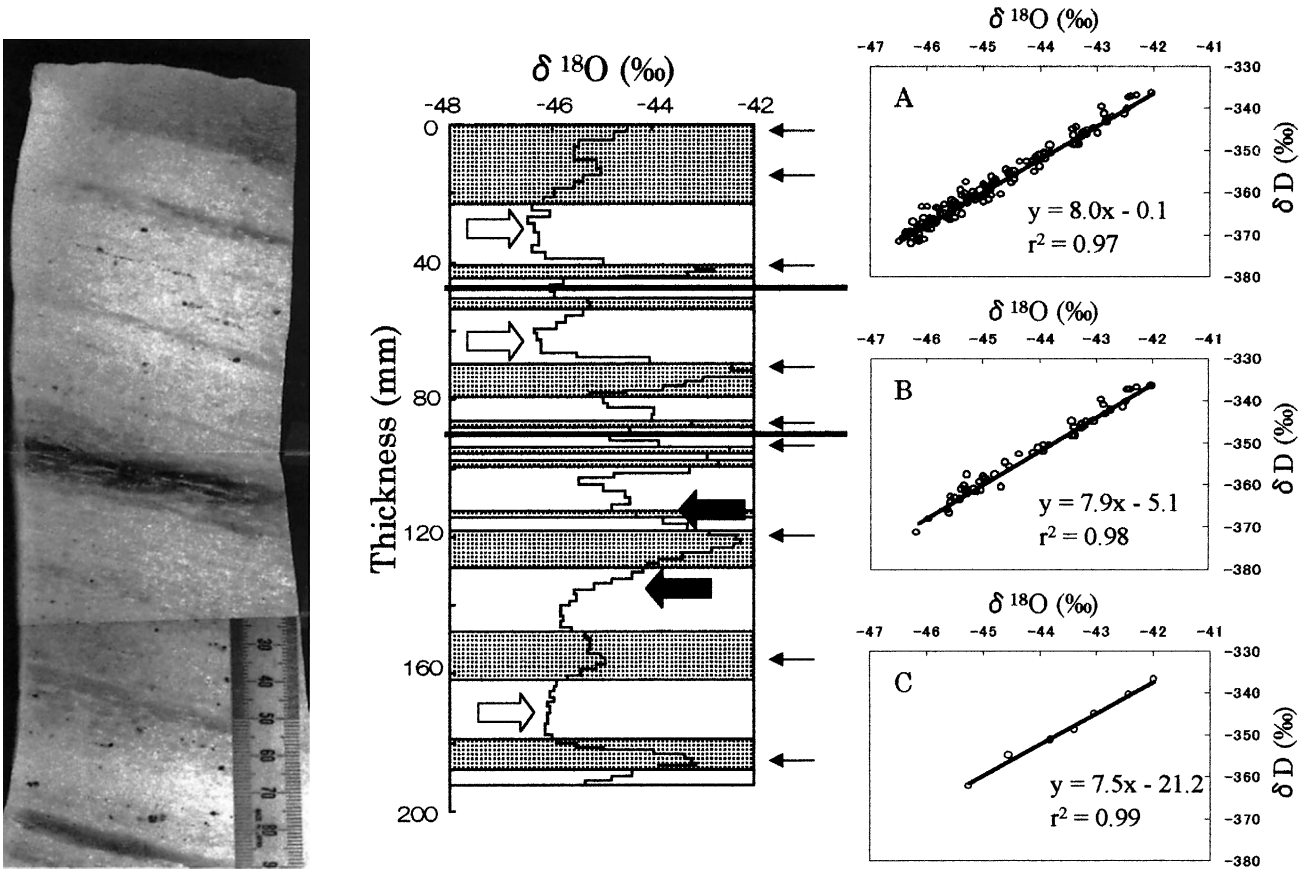

Fig. 8. A photograph and a vertical profile of $\delta^{18}O$ (‰) values of Basal Ice-E at about 1.7 m in height. The vertical axis, dotted squares, open squares, thin arrows and thick black arrows have the same meanings as in Figure 7. Thick white arrows show the bubbly ice layers having quasi-neutral values on the isotopic profile. Each value was measured through about a 1.5 mm thickness. Slopes of $\delta^{18}O$ vs δD of all the samples (A: 117 samples), of samples on the bubble-free ice (B: 50 samples), and of samples on a single decreasing line from 72 to 80 mm thickness (C: 7 samples) are also shown.

formed by freezing at the base of the ice sheet. The water that was frozen must have been meltwater from inland ice, because δ values as low as −45.6‰ ($\delta^{18}O$) and −364‰ (δD) are only available from the inland ice.

Relatively larger grain-size observed in the bubble-free layers as compared to that in the bubbly layers (Table 1; Fig. 4) supports the statement above because the grain-size of sheared layers is relatively smaller than that of associated bubbly layers if the bubble-free layers were formed by a mechanical process such as shearing (Tison and others, 1993). Our measurements do not fit this idea, so the bubble-free layers are considered to have been formed by freezing of meltwater at the base.

On the other hand, the bubbly layers in the upper part of the Hamna Basal Ice could have been formed by two different processes. The isotopic profiles obtained for the Basal Ice-D and -E showed see-saw-type variations consisting of multiple "$>$" shapes in which two kinds of patterns were observed (Figs 7 and 8).

The first is a neutral profile found in Basal Ice-E as indicated by thick white arrows in Figure 8. In the bubbly layers, the δ values are as constant as those observed in the overlying ice-sheet ice (Fig. 5). Such bubbly layers are suggested to be ice not affected by the melting and refreezing process, and are considered to be the same as the overlying ice-sheet ice. The neutral profile can most likely be explained by assuming that the bubbly layers were folded/sheared and embedded within the bubble-free layers without suffering any isotopic fractionations.

The second type of pattern is indicated by thick black arrows where the δ values decrease gradually from the neighboring bubble-free layers without any significant breaks (Figs 7 and 8). Each pattern of the second type could be formed by a single meltwater-refreezing event associated with formation of the neighboring bubble-free layer, resulting in dissolved gas being trapped in frozen ice (Hubbard, 1991).

From the interpretation of the mechanisms acting on the formation of both bubble-free and bubbly layers in the upper part of the Hamna Basal Ice, we believe that two different mechanisms, refreezing of meltwater (i.e. regelation or congelation) and tectonic deformation, were important in formation of the upper part. The two processes could only occur in the same profile if a subglacial tectonic disturbance was predated by multiple regelation/congelation layers, which will be explained in the final subsection of the discussion.

Formation process of the lower part of the Hamna Basal Ice

It is clear that the lower part of the Hamna Basal Ice has long been affected by the underlying bedrock since the concentration of debris in the layer is significantly higher than in the upper part (Fig. 3). The development of multiple-maximum fabric found in the lower part also indicates that the lower part of the basal ice has long been subjected to strong shear stress, which is typical at the base of the ice sheet. In the co-isotopic profile of the lower part (Basal Ice-C in Fig. 6), the major variation corresponds to the stratigraphy of bubbles, and the range of the fluctuation in δ values is 3.2‰ ($\delta^{18}O$) and 30‰ (δD), which is again similar to the fluctu-

https://doi.org/10.3189/172756501781832359 Published online by Cambridge University Press

ations observed in the upper part. This suggests that the lower part was also formed by refreezing of meltwater. Since the isotopic change occurred over a wider thickness than in the upper part, the refreezing of the lower part is considered to have occurred on a larger scale (>100 mm thickness) than that of the upper part (1–10 mm thickness).

Possible freezing conditions deduced from $\delta^{18}O$ vs δD plots

Jouzel and Souchez (1982) showed that for a closed system, where there is no water input or output, the slope gradient defined by $\delta^{18}O$ vs δD (hereinafter we call this the freezing slope) depends on the initial composition of the liquid admitted to freeze (equation 1 in Souchez and de Groote, 1985) and takes the value 4.2 in the case of −45.6‰ ($\delta^{18}O$) and −364‰ (δD). In contrast, the freezing slope depends on (1) the isotopic composition of the initial and input water, and (2) the ratio of input to freezing-rate coefficient, if the system is open (equation 3 in Souchez and de Groote, 1985). The freezing slope becomes similar between open and closed systems when the isotopic composition of the input water is not significantly different from that of the initial water or when the freezing rate is much higher than the input rate. On the other hand, the freezing slope is nearly 8 when the isotopic composition of the input water is significantly different from that of the initial water and when the ratio of input to freezing-rate coefficient is high.

The freezing slopes obtained for the various parts of the Hamna Basal Ice were as follows: 8.6 (entire profile; Fig. 5), 7.5 (Basal Ice-D; Fig. 7A) and 8.0 (Basal Ice-E; Fig. 8A). The latter two values are more significant because the correlation coefficients for the two cases were high ($r = 0.97$–0.99) as compared with that obtained for the entire profile ($r = 0.83$). This lower coefficient results from the rough sampling interval (100 mm) in the analysis of the entire profile. Namely, the scale of analysis containing several sets of the alternating layers is too coarse to investigate the causes of the isotopic fluctuation. Besides, even if we select the data solely from the bubble-free layers, the slopes become 7.6 (Basal Ice-D; Fig. 7B) and 7.9 (Basal Ice-E; Fig. 8B). Furthermore, the freezing slope of 7.5 was also obtained when we calculated it in the single decreasing profile from an interval 72–80 mm thick in Basal Ice-E (Fig. 8C). Therefore, we conclude that the bubble-free layers and part of bubbly layers were formed by the melting–refreezing process in an open system in which the input water is isotopically different from the initial water. The input water is considered to be isotopically lighter than the initial water, because almost all of the measured isotopic enrichments in the bubble-free ice layers should be much larger than those of the theoretical fractionation by freezing, if the input water was isotopically heavier.

Now a question may arise as to how the meltwater was produced and supplied to the production of the bubble-free and part of the bubbly layers in the Hamna Basal Ice. As far as the radio-echo soundings and model simulation applied to Sôya drainage basin are concerned, the basal temperature is below the pressure-melting point (e.g. Mae and Yoshida, 1987; Hansen and Greve, 1996). The modeled basal temperature is, however, very close to the fusion temperature and there might be a possibility of melting area in relation to either enhanced local stresses or impurities. One example is that Mae and Naruse (1978) attributed the recent rapid thinning of the ice sheet to local melting at the bottom of nearby Shirase drainage basin. We cannot determine the origin of the meltwater at the moment, but we expect that study of the basal ice from a chemical viewpoint may shed light on it.

There are a few examples of bubble-free layers enriched by 5–6‰ (for $\delta^{18}O$) and 45–50‰ (for δD) compared with the overlying bubbly layers. The enrichment values are much larger than those expected from theoretical considerations for the single melt–freeze process. The larger enrichment values can be ascribed to multiple melting and refreezing processes (Hubbard and Sharp, 1993) in the single bubble-free layer.

Formation history of the Hamna Basal Ice

The most probable interpretation of the origin of the Hamna Basal Ice is that it was formed by either regelation or congelation of meltwater in an open system at the base of the ice sheet in the inland region. Bulk co-isotopic analyses of the Hamna Basal Ice showed that the average isotopic values are −45.6‰ ($\delta^{18}O$) and −364‰ (δD), which are nearly equivalent to those obtained for the overlying ice-sheet ice (Fig. 5). This fact excludes the possibility that it is fossil ice like that found in the Greenland ice sheet (Souchez and others, 1994). In addition to similar δ values, the lower part of the Hamna Basal Ice has similar crystal-orientation fabrics to the upper parts. Therefore, the lower part is not ice that accreted at the sampled point in the Hamna Glacier region like that reported for Glacier de Tsanfleuron, Switzerland (Tison and Lorrain, 1987).

Regelation is possible when the ice-sheet sole meets a bedrock bump (Weertman, 1964; Robin, 1976) or within a water-vein network in the basal layer above a bump (Lliboutry, 1993). Congelation can be caused by either a difference in the basal thermal regime (Boulton, 1972), cooling in a water-filled cavity (Shoemaker, 1990) or by supercooled water (Lawson and others, 1998). As mentioned above, the bottom of the ice sheet in the Sôya drainage is supposed to be frozen. This means that regelation or congelation, which produces the Hamna Basal Ice, can only be caused by local "stress" or "impurity"-induced melting and freezing.

Weertman (1964) showed that regelation thickness by single refreezing cannot exceed several hundred mm. The thickness of each bubble-free layer in the Hamna Basal Ice was at most 100 mm for the upper part and more than several hundred mm for the lower part. Therefore, the upper part of the Hamna Basal Ice was probably formed either by the Weertman-type or by the Lliboutry-type regelations. The massive lower part of the Hamna Basal Ice was probably formed by congelation related to either a water-filled cavity or a change in the thermal regime on the local scale.

Field observations on the Lliboutry-type regelation within a vein network were reported at Engabreen (Jansson and others, 1996) and Glacier de Tsanfleuron (Hubbard and others, 2000). They interpreted an ice layer with little debris and with high content of dissolved cations as a Lliboutry-type regelation layer. Since the bubble-free ice layers in the upper part of the Hamna Basal Ice contain debris, they are considered to be formed by Weertman-type regelation with the help of input water.

Now, we must consider how the upper part of the Hamna Basal Ice became as thick as 5.5 m. Successive accretion by multiple regelations from the bottom cannot be a complete explanation because some of the bubbly layers are thought to have originated from the ice-sheet ice without suffering from

https://doi.org/10.3189/172756501781832359 Published online by Cambridge University Press

isotopic fractionations. Such a process is only possible by mechanical deformation, i.e. shearing/thrusting or folding.

In the case of the Hamna Basal Ice, our analytical evidence favors a folding mechanism rather than thrusting/shearing. Not all of the maxima of the isotopic profiles, which means the positions of frozen ice in the first stage, were observed at the uppermost part of the bubble-free layers as indicated by the thin arrows in Figures 7 and 8. This fact excludes the thrusting/shearing mechanism in which the bubble-free layers forming isotopic maxima at the uppermost part (Hubbard and Sharp, 1993) should thrust from the bottom of the ice sheet onto the overlying ice-sheet ice (see fig. 6 of Tison and others, 1993). Moreover, a part of the isotopic profiles in Basal Ice-D and -E shows symmetrical patterns across layers with respect to the thick horizontal axes indicated at thicknesses of 50 mm in Figure 7, and 48 and 90 mm in Figure 8. These features strongly suggest that Basal Ice-D and -E are examples of folding.

Finally, we propose a hypothesis for the formation history of the Hamna Basal Ice (Fig. 9). At first, bubble-free ice and part of the bubbly layers were formed somewhere inland in the Sôya drainage basin, probably related to the bedrock bump with the help of input water at the base of the ice sheet (Fig. 9-①). The layers flowed downward beyond the bedrock bumps, and suffered shear stress and folded without significant shearing/thrusting (Fig. 9-②). The folded layers suffered from compression, due probably to bedrock undulation or cold stiff ice at the terminus (Fig. 9-③). Then the layers suffered strong shear stress after the accretion of the massive lower part by congelation, as we observed at the ice cliff at the terminus (Fig. 9-④). Since the fabric in the lower part shows the same features as that in the upper part (Fig. 3), the lower part is suggested to have been formed before the action of strong shear stress.

CONCLUSIONS

The Hamna Basal Ice exhibits two peculiar stratigraphic features. One is the upper part of the basal ice (height: 1.3–6.8 m), which consists of alternating layers of bubble-free and bubbly ice of the order of mm to cm in thickness and has a low concentration (<1% in weight) of dispersed debris. The other is the lower part of the basal ice (height: 0–1.3 m), which consists predominantly of bubble-free ice and has a high concentration (<4% in weight) of stratified debris. Isotopic analyses of the bulk samples show that the Hamna Basal Ice originated from precipitation in inland regions of the ice sheet. Based on estimation from the δ values, the Hamna Basal Ice could have originated from precipitation in the inland area around 3000 m a.s.l., about 150 km southeast of Mizuho station (70°42′ S, 44°20′ E).

We have presented the formation processes of the alternating layers in the upper part using detailed co-isotopic values. The bubble-free ice layers show smooth profiles for stable isotopes, with variations closely corresponding to values for theoretical fractionation of water to ice (Jouzel and Souchez, 1982), i.e. heavier δ values of 2.4 ± 1.0‰ and 19 ± 8‰ for $\delta^{18}O$ and δD, respectively, were observed in the bubble-free ice layers as compared with the neighboring bubbly ice layers. Since the freezing slopes of the layers are close to 8, such layers are suggested to have been formed by refreezing of meltwater in an open system (Souchez and Jouzel, 1984;

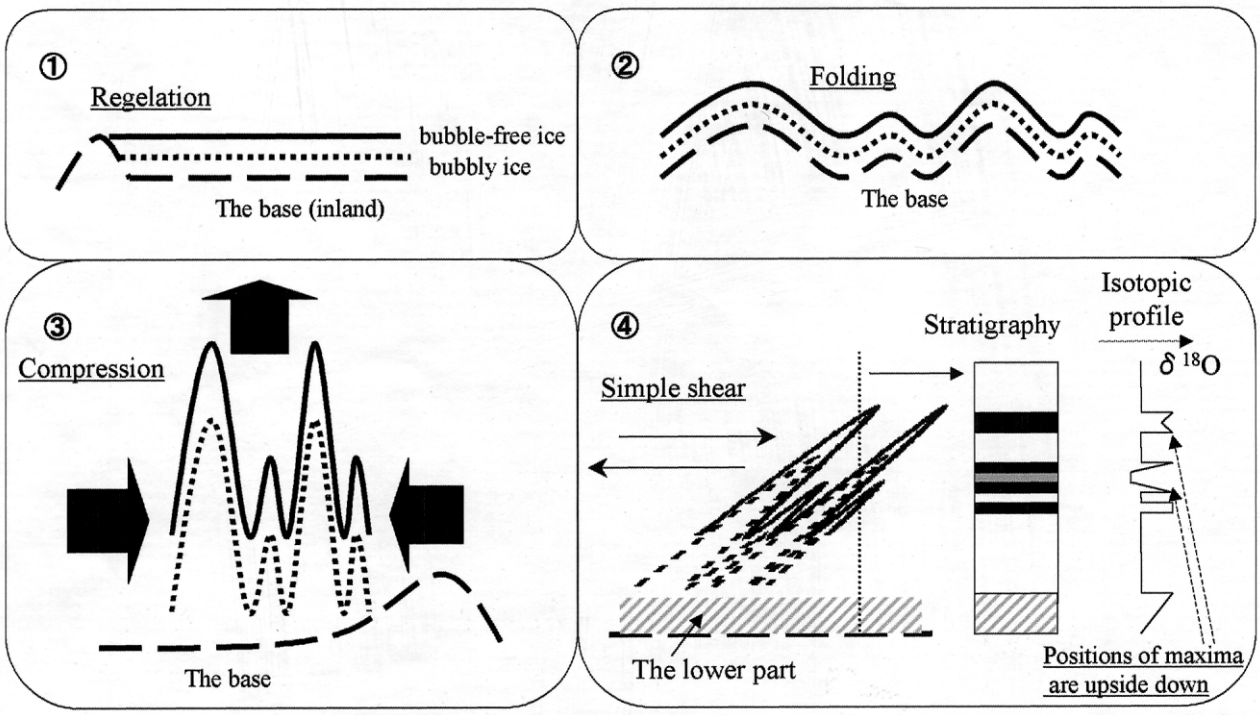

Fig. 9. Schematic diagrams on the formation history of the Hamna Basal Ice. ①: Bubble-free and bubbly ice layers were formed by regelation at bumps in the inland region of the Sôya drainage. The layers between the solid line and the short-period dotted line, and between the dotted and dashed lines, show the bubble-free ice and the bubbly ice layers formed by regelation. For the sake of simplicity, we consider here one regelation layer only; ②: After the regelation layers were folded parallel to bed topography; ③: Then the folded layers were thickened by compressive stress near the terminal area; ④: The thickened layers were finally subjected to simple shear to form a recumbent fold. Also shown are the stratigraphy of bubbles and the associated isotopic profile. The stratigraphy is a schematic section cut vertically to the base to visualize the stratigraphy of the actual Hamna Basal Ice. In this section, bubbly ice originating from ice-sheet ice is represented by white spaces, bubbly ice originated from subglacial water by gray spaces, bubble-free ice of the upper part by black spaces, and bubble-free ice of the lower part by slant-lined spaces.

https://doi.org/10.3189/172756501781832359 Published online by Cambridge University Press

Souchez and de Groote, 1985). The mechanism of the freezing is probably regelation at a bed bump. On the other hand, a part of the bubbly layers shows neutral profiles for stable isotopes, with values closely corresponding to the overlying ice-sheet ice. Such bubbly layers are suggested not to have been affected by the melt–freezing process. The alternating layers are considered to have been formed by piling up of freezing layers and non-melted layers followed by folding.

The profile of stable isotopes in the lower part shows variations similar to those observed in the upper part. The range of the fluctuation in δ values was 3.2‰ for $\delta^{18}O$ and 30‰ for δD. Since the isotopic fluctuation was found to have occurred on a larger scale in the lower part (>100 mm thickness), the freezing mechanism of the lower part is probably congelation in a water-filled cavity or congelation by a change in the basal thermal regime on a local scale.

ACKNOWLEDGEMENTS

We would like to thank K. Yokoyama of Hokuriku National Agricultural Experiment Station and the members of the 35th Japanese Antarctic Research Expedition for their support in the field operation and sampling of ice. We are grateful to O. Watanabe and Y. Fujii of the National Institute of Polar Research for useful discussion of this study. The paper was significantly improved as a result of comments by M. J. Sharp and an anonymous referee to whom we are greatly indebted.

REFERENCES

Alley, R. B., D. E. Lawson, E. B. Evenson, J. C. Strasser and G. J. Larson. 1998. Glaciohydraulic supercooling: a freeze-on mechanism to create stratified, debris-rich basal ice. II. Theory. *J. Glaciol.*, **44**(148), 563–569.

Boulton, G. S. 1972. The role of thermal régime in glacial sedimentation. *In* Price, R.J. and D.E. Sugden, *comps. Polar geomorphology.* London, Institute of British Geographers, 1–19.

Bouzette, A. and R. Souchez. 1999. Katabatic wind influence on meltwater supply to fuel glacier–substrate interactions at the grounding line, Terra Nova Bay, East Antarctica. *Ann. Glaciol.*, **28**, 272–276.

Craig, H. 1961. Isotopic variations in meteoric waters. *Science*, **133**(3465), 1702–1703.

Fitzsimons, S. J. 1996. Formation of thrust-block moraines at the margins of dry-based glaciers, south Victoria Land, Antarctica. *Ann. Glaciol.*, **22**, 68–74.

Goodwin, I. D. 1993. Basal ice accretion and debris entrainment within the coastal ice margin, Law Dome, Antarctica. *J. Glaciol.*, **39**(131), 157–166.

Gow, A. J., S. Epstein and W. Sheehy. 1979. On the origin of stratified debris in ice cores from the bottom of the Antarctic ice sheet. *J. Glaciol.*, **23**(89), 185–192.

Hansen, I. and R. Greve. 1996. Polythermal modelling of steady states of the Antarctic ice sheet in comparison with the real world. *Ann. Glaciol.*, **23**, 382–387.

Hubbard, B. 1991. Freezing-rate effects on the physical characteristics of basal ice formed by net adfreezing. *J. Glaciol.*, **37**(127), 339–347.

Hubbard, B. and M. Sharp. 1993. Weertman regelation, multiple refreezing events and the isotopic evolution of the basal ice layer. *J. Glaciol.*, **39**(132), 275–291.

Hubbard, B. and M. Sharp. 1995. Basal ice facies and their formation in the western Alps. *Arct. Alp. Res.*, **27**(4), 301–310.

Hubbard, B., J.-L. Tison, L. Janssens and B. Spiro. 2000. Ice-core evidence of the thickness and character of clear-facies basal ice: Glacier de Transfleuron, Switzerland. *J. Glaciol.*, **46**(152), 140–150.

Jansson, P., J. Kohler and V. A. Pohjola. 1996. Characteristics of basal ice at Engabreen, northern Norway. *Ann. Glaciol.*, **22**, 114–120.

Jouzel, J. and R. A. Souchez. 1982. Melting–refreezing at the glacier sole and the isotopic composition of the ice. *J. Glaciol.*, **28**(98), 35–42.

Kato, K. 1979. [Oxygen isotopic composition of fallen snow in Antarctica.] *Antarct. Rec.* 67, 124–135. [In Japanese with English summary.]

Kizaki, K. 1962. Icefabric studies on Hamna ice fall and Honhörbrygga Glacier, Antarctica. *Antarct. Rec.* 16, 54–74.

Kluiving, S. J., L. R. Bartek and F. M. van der Wateren. 1999. Multi-scale analyses of subglacial and glaciomarine deposits from the Ross Sea continental shelf, Antarctica. *Ann. Glaciol.*, **28**, 90–96.

Knight, P. G. 1987. Observations at the edge of the Greenland ice sheet: boundary condition implications for modellers. *International Association of Hydrological Sciences Publication* 170 (Symposium at Vancouver 1987 — *The Physical Basis of Ice Sheet Modelling*), 359–366.

Knight, P. G. 1994. Two-facies interpretation of the basal layer of the Greenland ice sheet contributes to a unified model of basal ice formation. *Geology*, **22**(11), 971–974.

Lawson, D. E. 1979. Sedimentological analysis of the western terminus region of the Matanuska Glacier, Alaska. *CRREL Rep.* 79-9.

Lawson, D. E., J. C. Strasser, E. B. Evenson, R. B. Alley, G. J. Larson and S. A. Arcone. 1998. Glaciohydraulic supercooling: a freeze-on mechanism to create stratified, debris-rich basal ice. I. Field evidence. *J. Glaciol.*, **44**(148), 547–562.

Lehmann, M. and U. Siegenthaler. 1991. Equilibrium oxygen- and hydrogen-isotope fractionation between ice and water. *J. Glaciol.*, **37**(125), 23–26.

Lliboutry, L. 1993. Internal melting and ice accretion at the bottom of temperate glaciers. *J. Glaciol.*, **39**(131), 50–64.

Mae, S. and R. Naruse. 1978. Possible causes of ice sheet thinning in the Mizuho Plateau. *Nature*, **273**(5660), 291–293.

Mae, S. and M. Yoshida. 1987. Airborne radio echo-sounding in Shirase Glacier drainage basin, Antarctica. *Ann. Glaciol.*, **9**, 160–165.

Ohba, T. and J. Hirabayashi. 1996. Handling of Pt catalyst in H_2-H_2O equilibration method for D/H measurement of water. *Geochem. J.*, **30**, 373–377.

O'Neil, J. R. 1968. Hydrogen and oxygen isotope fractionation between ice and water. *J. Phys. Chem.*, **72**(10), 3683–3684.

Robin, G. de Q. 1976. Is the basal ice of a temperate glacier at the pressure melting point? *J. Glaciol.*, **16**(74), 183–196.

Satow, K. and O. Watanabe. 1992. Distribution of mean $\delta^{18}O$ values of surface snow layers and their dependence on air temperature in Enderby Land–East Queen Maud Land, Antarctica. *Proc. NIPR Symp. Polar Meteorol. Glaciol.* 5, 120–127.

Shoemaker, E. M. 1990. A subglacial boundary-layer regelation mechanism. *J. Glaciol.*, **36**(124), 263–268.

Souchez, R. A. and J. M. de Groote. 1985. δD–$\delta^{18}O$ relationships in ice formed by subglacial freezing: paleoclimatic implications. *J. Glaciol.*, **31**(109), 229–232.

Souchez, R. A. and J. Jouzel. 1984. On the isotopic composition in δD and $\delta^{18}O$ of water and ice during freezing. *J. Glaciol.*, **30**(106), 369–372.

Souchez, R., J.-L. Tison and J. Jouzel. 1987. Freezing rate determination by the isotopic composition of the ice. *Geophys. Res. Lett.*, **14**(6), 599–602.

Souchez, R. *and 8 others*. 1994. Stable isotopes in the basal silty ice preserved in the Greenland ice sheet at Summit: environmental implications. *Geophys. Res. Lett.*, **21**(8), 693–696.

Sugden, D. E. *and 6 others*. 1987. Evidence for two zones of debris entrainment beneath the Greenland ice sheet. *Nature*, **328**(6127), 238–241.

Tison, J.-L. and R. D. Lorrain. 1987. A mechanism of basal ice-layer formation involving major ice-fabric changes. *J. Glaciol.*, **33**(113), 47–50.

Tison, J.-L., J.-R. Petit, J.-M. Barnola and W. C. Mahaney. 1993. Debris entrainment at the ice–bedrock interface in sub-freezing temperature conditions (Terre Adélie, Antarctica). *J. Glaciol.*, **39**(132), 303–315.

Weertman, J. 1964. The theory of glacier sliding. *J. Glaciol.*, **5**(39), 287–303.

Zdanowicz, C. M., F. A. Michel and W. W. Shilts. 1996. Basal debris entrainment and transport in glaciers of southwestern Bylot Island, Canadian Arctic. *Ann. Glaciol.*, **22**, 107–113.

MS received 4 January 2000 and accepted in revised form 29 January 2001